Isolation and Characterization of Nitric Oxide Reductase from *Paracoccus halodenitrificans*†

Nobuhiko Sakurai and Takeshi Sakurai*

Institute for Molecular Science, Okazaki National Research Institutes, Myodaiji, Okazaki 444, Japan

Received May 7, 1997; Revised Manuscript Received August 21, 1997⊗

ABSTRACT: Nitric oxide reductase was isolated from the membrane fraction of a denitrifying bacterium, *Paracoccus halodenitrificans*, in the presence of *n*-dodecyl β-D-maltoside. A relatively simple and effective procedure to purify NO reductase using DEAE-Toyopearl and hydroxyapatite (ceramic) chromatographies has been developed. The enzyme consisted of two subunits with molecular masses of 20 and 42 kDa associated with the *c*-type heme and two *b*-type hemes, respectively. The optical and magnetic circular dichroism (MCD) spectra of the oxidized (as isolated) and reduced enzymes indicated that the heme *c* is in the low-spin state and the hemes *b* are in the high- and low-spin states. The EPR spectrum also showed the presence of the split high-spin component ($g_\perp = 6.6, 6.0$) and two low spin components ($g_{z,y,x} = 2.96, 2.26, 1.46$, $g_z = 3.59$). Although the presence of an extra iron was suggested from atomic absorption spectroscopy, a non-heme iron could not be detected by colorimetric titrations using ferene and 2-(5-nitro-2-pyridylazo)-5-(*N*-propyl-*N*-sulfopropylamino)phenolate (PAPS). One of the extra signals at $g = 4.3$ and 2.00 might come from a non-heme iron, while they may originate from an adventitious iron and a certain nonmetallic radical, respectively. When CO acted on the reduced enzyme, both of the low-spin hemes were not affected, and when NO acted on the reduced enzyme, the optical and MCD spectra were of a mixture of the oxidized and reduced enzymes. Consequently, the reduction of NO was supposed to take place at the high-spin heme *b*. The heme *c* and the low-spin heme *b* centers were considered to function as electron mediators during the intermolecular and intramolecular processes.

Denitrification is the process in which nitrate is reduced to nitrogen through nitrite, nitric oxide, and nitrous oxide (Berks et al., 1995; Averill, 1996):

$$NO_3^- \rightarrow NO_2^- \rightarrow NO \rightarrow N_2O \rightarrow N_2$$

A variety of metalloenzymes are involved in this series of reduction steps. Nitrate reductase is a membrane-bound enzyme containing molybdopterin, heme *b*, and an iron−sulfur center, all of which are necessary to produce enzyme activity (Berks et al., 1994; Lu et al., 1995). Nitrite oxidase also has the same set of active sites. There are two types of nitrite reductases, the copper enzyme (Masuko et al., 1984) and cytochrome cd_1 enzyme (Moir et al., 1993; Palmedo et al., 1995; Yamazaki et al., 1995). The former contains three type 1 and three type 2 coppers in a trimer complex (Godden et al., 1991). Although the copper and iron enzymes have quite different structures, they show the same enzyme activity. There had been doubt about the presence of NO reductase. However, the controversy in recent years whether or not NO is a free obligatory intermediate in the denitrification pathway, or whether nitrite reductase produces nitrous oxide directly from nitrite without producing NO (Averill & Tiefje, 1982), has been solved by the recent discovery of NO reductase (Zumft & Vega, 1979; Carr et al., 1989; Turk & Hollocher, 1992). Nitrous oxide reductase is a copper enzyme whose characterization is also in progress (Matsubara & Zumft, 1982).

The reasons why the presence of NO reductase was not ascertained for a long time are that this enzyme is an unstable membrane-bound protein (Matsubara & Iwasaki, 1971) and the gas sensitive to dioxygen has to be treated in the enzyme assay (Frunzke & Zumft, 1984; Bell et al., 1992; Zimmer et al., 1985). However, NO reductase has been discovered in denitrifying bacteria such as *Pseudomonas stutzeri* (Heiss et al., 1989), *Paracoccus denitrificans* (formerly named *Thiosphaera pantotropha*) (Carr & Ferguson, 1990; Dermastia et al., 1991; Fujiwara & Fukumori, 1996; Girsch & de Vries, 1997), *Achromobacter cycloclastes* (Jones & Hollocher, 1993), *Pseudomonas perfectomarinus* (Zumft & Vega, 1979), *Rhodobacter capsulatus* (Bell et al., 1992), and *Paracoccus halodenitrificans* (Grant et al., 1984). All of these NO reductases have been revealed to have the heme *b* and heme *c* centers. However, NO reductase is still the least characterized enzyme involved in denitrification, and its spectroscopic and molecular characterizations have not been satisfactorily developed because of purification difficulty and poor yield, although the study on the P-450 type NO reductase from *Fusarium oxysporum* has been rapidly advanced (Shiro et al., 1995).

Together with nitrous oxide reductase, NO reductase has received special attention, since these two enzymes are supposed to be the precursor of the terminal oxidases such as cytochrome oxidase and ubiquinol oxidase (Antholine et al., 1992; Saraste & Castresana, 1994). Therefore, the structural, mechanistic, and genetic aspects of NO reductase are significantly correlated with a wide range of respiration systems. In addition, the physiological reduction process of

† This research was supported by a Grant-in-Aid for Scientific Research on Priority Areas (08249214) from the Ministry of Education, Science, Sports and Culture of Japan.

* To whom correspondence should be addressed.

⊗ Abstract published in *Advance ACS Abstracts,* October 15, 1997.

S0006-2960(97)01070-2 CCC: $14.00

NO, one of the most interesting molecules as a novel hormone, has not been fully understood compared to its oxidation process.

In the present paper we show a new and relatively simple procedure to purify NO reductase from *Paracoccus halodenitrificans* and describe its spectroscopic characterization using absorption, MCD,[1] and EPR spectroscopies. We characterize the three heme centers by using these spectroscopies and discusse their biological roles.

MATERIALS AND METHODS

Organism, Growth Conditions, and Membrane Preparations. Paracoccus halodenitrificans IFO 14912 was obtained from the Institute for Fermentation, Osaka, Japan, and was stationarily grown at 30 °C in medium containing 5 g of polypeptone, 3 g of meat extract, 60 g of sodium chloride, 5 g of sodium DL-lactate, 10 g of potassium nitrate, 1 g of magnesium sulfate, 0.02 g of iron(III) chloride, and 0.17 mg of copper(II) chloride per liter (pH 6.5). Nitrogen gas passed through a bactericidal filter was gently bubbled into the medium at the final culture. Cells were harvested by continuous centrifugation at 4000*g* and washed in 20 mM Tris-HCl containing 1.0 M sodium chloride, pH 8.0. About 6.5 g (wet weight) of cells were obtained per liter of medium; they were stored at −50 °C until use.

The cells (90 g) were suspended in ca. 8-fold volume of 0.02 M Tris-HCl, pH 8.0, containing 0.1 mM EDTA, 0.1 mM PMSF, 0.01% 2-phenylethanol, 0.25 mM benzamidine (buffer A), and 0.6 g of lysozyme from egg white. After gentle stirring for 30 min, DNase was added at 2 μg/mL and sonicated for 3 min (duty cycle, 90%; output, ca. 180 W) for five times, carefully avoiding an increase in temperature. Broken cells were centrifuged at 4000*g* for 20 min, and after unbroken cells and heavy debris were removed, the resulting cell-free extract was centrifuged at 130000*g* for 1.5 h. The pellet was washed with buffer A and centrifuged. The suspended pellet could be stored at −50 °C for several months.

Detergent and Solubilization of the Membrane Proteins. The detergent for extraction and solubilization of the membrane fractions was screened among *n*-dodecyl β-D-maltoside, octyl glucoside, SM-1000 (sucrose monocaprate, Mitsubishi-Kasei Foods), SM-1200 (sucrose monolaurate, Mitsubishi-Kasei Foods), digitonin, MEGA-8, MEGA-9, BIGCHAP, deoxy-BIGCHAP, *n*-heptyl β-D-thioglucoside, and CHAPSO (protein and detergent concentrations were adjusted to 5 mg/mL and centrifuged to obtain the solubilized fractions). While NO reductase was almost not solubilized by CHAPSO, it was effective for washing out the other membrane components with the least loss of NO reductase activity (84% recovery). Therefore, we treated the membrane fractions with CHAPSO for 30 min before solubilizing the NO reductase. The enzyme activity was increased by 150%, 90%, and 50% compared to the activity of the membrane fraction when treated with *n*-dodecyl β-D-maltoside, SM-1200, and SM-1000, respectively. However, all other detergents were not very effective in solubilizing the membrane fractions. Therefore, *n*-dodecyl β-D-maltoside was used throughout the preparation and measurements.

Purification. The membrane fractions (2840 mg) treated with CHAPSO were centrifuged at 130000*g* for 1.5 h. The precipitate was washed with buffer A and homogenized in a minimal amount of buffer. *n*-Dodecyl β-D-maltoside (the same amount as the total protein of 5 mg/mL concentration) was slowly added onto the CHAPSO-treated membrane fractions and then stirred gently for 30 min. The solubilized membrane fractions were centrifuged at 130000*g* for 1.5 h, and buffer A (4 times the volume) was added. The supernatant was subjected to anion-exchange chromatography on DEAE-Toyopearl (Tosoh) (2.5 × 50 cm) previously equilibrated with buffer A containing 0.05% *n*-dodecyl β-D-maltoside. Proteins were adsorbed on the top of the column, followed by the washing with the same buffer containing 0.15 M NaCl. Proteins were eluted with a buffered linear NaCl gradient from 0.15 to 0.4 M (total volume, 1000 mL). Fractions high in NO reductase activity were obtained at around 0.3 M NaCl. Although fractions with NO reductase activity were also obtained at higher NaCl concentrations, their specific activities were relatively low and the R_f value on native PAGE was different from the first fractions. Therefore, only the main fractions were collected and dialyzed against 20 mM Tris-HCl buffer (pH 8.0) containing 0.02% *n*-dodecyl β-D-maltoside, 0.01% 2-phenylethanol, and 0.25 mM benzamidine (buffer B). Subsequently, the second DEAE-Toyopearl chromatography (1.5 × 30 cm) was performed with a buffered linear NaCl gradient from 0.2 to 0.35 M. The fractions eluted at ca. 0.27 M NaCl were dialyzed against 0.1 M phosphate buffer (pH 7.0) containing 0.02% *n*-dodecyl β-D-maltoside, 0.01% 2-phenylethanol, and 0.25 mM benzamidine (buffer C). From these anion-exchange chromatographies an ca. 7-fold purification was attained. The ceramic hydroxyapatite chromatography (Bio-Scale CHT 20-I, 1.5 × 11.3 cm) was then performed with a linear gradient from 0.1 to 1 M phosphate buffer containing 0.01% 2-phenylethanol and 0.05% *n*-dodecyl β-D-maltoside (pH 7.0). NO reductase was eluted with a 0.7−0.8 M buffer concentration. While two peaks with NO reductase were noticeable in the elution profile, the second one was collected and dialyzed against buffer C. From this hydroxyapatite chromatography, NO reductase was purified 55-fold in one step. The second hydroxyapatite chromatography was performed to remove the small amount of impurity. NO reductase was dialyzed against buffer B and concentrated using DEAE-Toyopearl (1 mL) equilibrated with 20 mM Tris-HCl buffer (pH 8.0) containing 0.05% *n*-dodecyl β-D-maltoside, 0.01% 2-phenylethanol, and 0.25 mM benzamidine. NO reductase was eluted with a minimum volume of the same buffer containing 0.5 M NaCl. EDTA (1 mM) was added to the concentrated NO reductase. After incubating overnight, the NO reductase was dialyzed against 20 mM HEPES-NaOH (pH 7) containing 0.01% 2-phenylethanol, 0.25 mM benzamidine, and 0.05% *n*-dodecyl β-D-maltoside.

Assays. Reaction vessels (12.8 mL volume) attached to a Teflon stopcock for evacuation were used for the enzyme assay. The reaction mixture (total volume, 3.0 mL) contains 0.3 mL of the enzyme sample, 50 μmol of sodium ascorbate, 0.5 μmol of PMS (Zumft & Frunzke, 1982), 300 μmol of D-glucose, 2.4 units of D-glucose oxidase, 60 units of catalase (Fujiwara & Fukumori, 1996), and 1 μmol of EDTA in 83

[1] Abbreviations: MCD, magnetic circular dichroism; PMSF, phenylmethanesulfonyl fluoride; PMS, phenazine methosulfate; MEGA-8, octanoyl *N*-methylglucamide; MEGA-9, nanoyl *N*-methylglucamide; BIGCHAP, *N*,*N*-bis[3-D-glucoamidopropyl]cholamide; CHAPSO, 3-[(3-cholamidopropyl)dimethylammonio]-2-hydroxy1-propanesulfonate; PAPS, 2-(5-nitro-2-pyridylazo)-5-(*N*-propyl-*N*-sulfopropylamino)phenolate.

Table 1: Purification of *Paracoccus halodenitrificans* NO Reductase

purification stage	volume (mL)	total protein (mg)	total activity (units)	specific activity (units min^{-1} mg^{-1})	yield (%)	purification (*x*-fold)
membrane fraction	307	2840	887	0.312	100	1
CAPSO ppt	180	1730	746	0.431	84.1	1.38
n-dodecyl β-D-maltoside treatment	395	1000	554	0.554	62.5	1.78
1st DEAE-Toyopearl	102	101	170	1.68	19.2	5.38
2nd DEAE-Toyopearl	21.1	37.3	80.4	2.16	9.06	6.92
1st BIO-Scale CHT20-1	53.1	2.75	47.1	17.1	5.31	54.8
2nd BIO-Scale CHT20-1	12.5	1.01	22.4	22.2	2.53	71.2

mM sodium acetate buffer (pH 5.0). After successive evacuation and flushing with Ar, *n*-dodecyl β-D-maltoside (0.02%) was introduced through a rubber septum and the sample was evacuated again. Finally, the reaction was started by introducing a NO−Ar mixture (5% NO content) into the reaction vessel followed by shaking at 30 °C. At an appropriate time interval, 0.1 mL of the gas was sampled using a Hamilton gastight syringe and quantified by gas chromatography. Both the reduction of NO and the formation of N_2O were followed (Frunzke & Zumft, 1984) using Molecular Sieves 5A (2 m · 3 mm i.d.; Yanaco) at 40 °C and Porapack Q (3.5 m · 3 mm i.d.; Waters) at 55 °C on a gas chromatograph with a thermal conducting detector, respectively. Helium was used as the carrier gas at a pressure of 1.6 kg/cm^2 for NO and 0.8 kg/cm^2 for N_2O detections. One unit of activity corresponds to 1 μmol of NO consumed/min. Cytochrome oxidase activity was measured according to the literature (Matsushima et al., 1982).

Hemes were analyzed by the pyridine ferrohemochrome (Dispirito, 1990) method using myoglobin and horse heart cytochrome *c* as standards (Berry & Trumpower, 1987). Nonheme iron was examined using the ferene method (Hennessy et al., 1984) and nitro-PAPS method (Makino et al., 1988). The total amount of iron in a protein molecule was determined by atomic absorption spectroscopy.

Measurements. Absorption spectra were measured on a Shimadzu UV-3100 spectrometer or on a Jasco Ubest-50 spectrophotometer. MCD spectra were obtained on a Jasco J-720W spectropolarimeter equipped with an electromagnet at a magnetic field of 1.4 T. EPR spectra were measured with a Bruker ESP-300E spectrometer attached to an Oxford liquid helium cryostat at 3−20 K. Gas chromatography was performed on a Yanaco G-2800 that was previously calibrated by injecting known amounts of NO and N_2O before the measurements. Atomic absorption spectroscopy has been performed on a Shimadzu AA-6200 spectrophotometer.

RESULTS

NO reductase was purified from the membrane fractions of anaerobically grown *P. halodenitrificans* in the presence of the detergent, *n*-dodecyl β-D-maltoside, by anion-exchange column-chromatography and low-pressure liquid chromatography on hydroxyapatite (Table 1). By carefully selecting the anion-exchange resin and hydroxyapatite, we could minimize protein smearing on the columns and realize a highly reproducible preparation of the enzyme. The elution profiles from the first DEAE-Toyopearl chromatography and Bio-Rad ceramic hydroxyapatite chromatography are shown in Figures 1 and 2, respectively.

The activity of *P. halodenitrificans* NO reductase was similar to that from *Ps. stutzeri* (Heiss et al., 1989). This enzyme also showed weak cytochrome oxidase activity (2.6 units/mg) similar to that reported from *P. denitrificans* (Fujiwara & Fukumori, 1996).

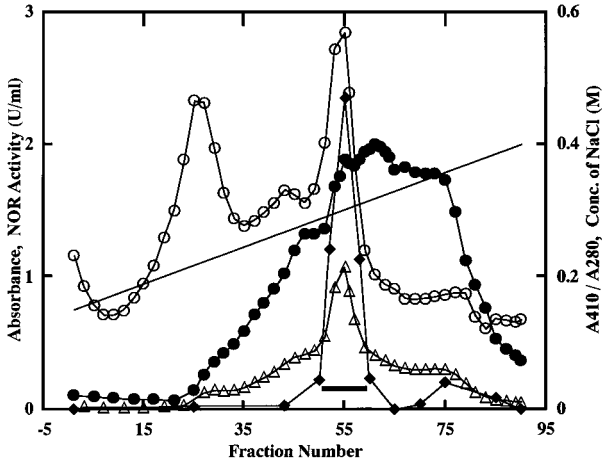

FIGURE 1: Elution profile of NO reductase on the first DEAE-Toyopearl column. Conditions were described in Materials and Methods in detail. ●, △, ○, and ◆ represent A_{280}, A_{410}, A_{410}/A_{280}, and NO reductase activity, respectively. The bold line under the peak shows the fractions collected.

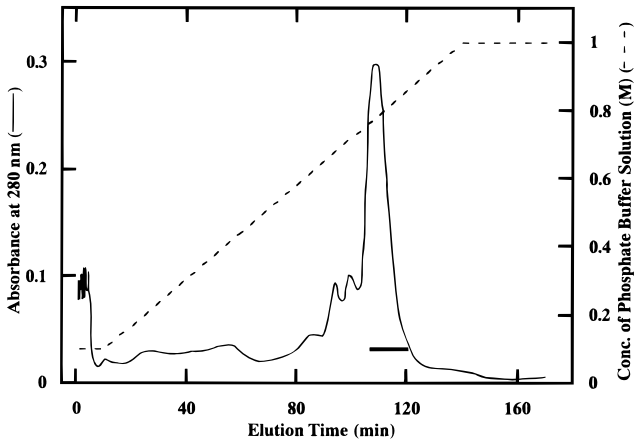

FIGURE 2: Elution profile of NO reductase on the first hydroxyapatite column. Conditions were described in Materials and Methods in detail. The bold line under the peak shows the fractions collected.

Purified NO reductase was homogeneous on native PAGE (not shown). SDS−PAGE (Figure 3) showed two bands with apparent molecular masses of 20 and 42 kDa, indicating that the two subunits are complexed (the pale band for 66.5 kDa came from the complexed form of NO reductase or from aggregated subunits). On the basis of heme staining, the former subunit was found to have a covalently bound *c*-type heme. On the other hand, heme was eliminated from the latter subunit by incubating at 80 °C for 5 min because the contained heme is not the *c* type.

According to the heme determination by the pyridine ferrohemochrome method the noncovalently bound heme was

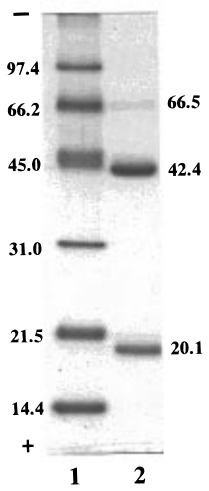

FIGURE 3: SDS−PAGE of NO reductase. SDS−PAGE was performed at 6 °C in a linear gradient of 15−25% polyacrylamide. The enzyme (2 μg of protein) was treated with 2% SDS and 5% 2-mercaptoethanol at 40 °C for 5 min and loaded onto a polyacrylamide gel. Lanes: 1, standard proteins (rabbit muscle phosphorylase *b*, BSA, hen egg white ovalbumin, bovine carbonic anhydrase, soybean trypsin inhibitor, and hen egg white lysozyme); 2, purified NO reductase. The molecular masses (kilodaltons) are shown on the side of lanes. The pale band at 66.5 kDa came from an intact complexed form of NO reductase or aggregated subunits.

found to be the *b* type, judging from the wavelength for the α band (Yamanaka, 1988). In addition, the content of heme *b* and heme *c* was in a 2.1:1 ratio or approximately 2 to 1. The colorimetric determinations of non-heme iron showed only a trace amount of non-heme iron differing from results for *P. denitrificans* and *Ps. stutzeri* NO reductases (Heiss et al., 1989; Fujiwara & Fukumori, 1996; Girsch & de Vries, 1997). However, atomic absorption spectroscopy showed the presence of 3.6 Fe atoms in a protein molecule, indicating that one non-heme iron might be contained in the NO reductase. Copper was never detected in the final enzyme preparation.

Figure 4 shows the absorption and MCD spectra of the oxidized (as isolated) and the reduced (dithionite) NO reductase. The Soret band with a maximum at 410 nm for the oxidized form and at 419 nm for the reduced form is characteristic of a heme protein. While the oxidized enzyme gave the three broad bands at ca. 526, ca. 560, and ca. 595 nm in the Q band region, the reduced enzyme showed a sharp band at 552 nm, being accompanied by a shoulder at ca. 560 nm as for the α bands. In the β band region, three bands were noticeable at ca. 512 (shoulder), 522, and 532 (shoulder) nm for the reduced NO reductase. The sharpening and increase in intensity of the α bands at 552 and ca. 560 nm upon reduction strongly suggests that the absorbance maxima belong to the low-spin hemes *c* and *b*, respectively (Fujiwara & Fukumori, 1996). Since another heme *b* did not show a sharp peak in the reduced form, it was supposed to be in the high-spin state. The broad maximum at around 595 nm in the oxidized enzyme has recently been assigned to the high-spin heme *b* in the *P. denitrificans* NO reductase (Makinen & Chung, 1983; Girsch & de Vries, 1997).

The MCD spectrum of the reduced enzyme was apparently composed of three components. In the α band region, two derivative-shaped bands centered at ca. 551 and ca. 556 nm were superimposed. On the negative-sign band at ca. 555 nm were superimposed the strong negative-sign band and a

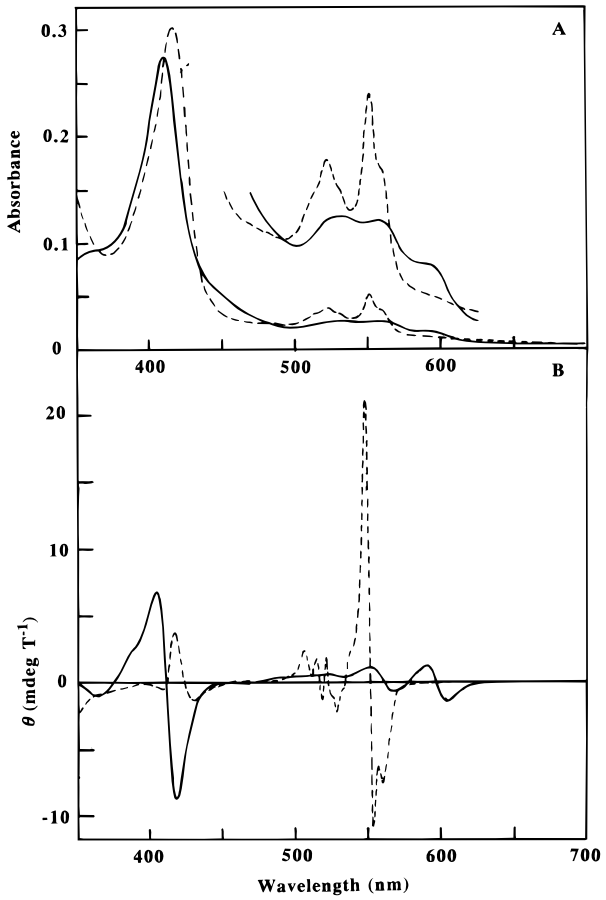

FIGURE 4: Absorption (A) and MCD (B) spectra of NO reductase in the oxidized (solid line, as isolated) and reduced (broken line, dithionite) forms. Purified NO reductase (0.109 mg of protein/mL) was dissolved in 20 mM HEPES-NaOH buffer (pH 7.0) containing 0.05% *n*-dodecyl β-D-maltoside, 0.01% 2-phenylethanol, and 0.25 mM benzamidine.

positive-sign band, which are coupled with the positive-sign band at ca. 547 nm and the negative-sign band at ca. 560 nm, respectively. These derivative-shaped bands are typical of low-spin hemes (Ookubo et al., 1987). Therefore, these two bands originate in the low-spin heme *c* and the low-spin heme *b*, respectively. On the other hand, the spectral feature of the Soret band and its appearance at a relatively long wavelength region indicated that a high-spin heme was also present.

The features of the MCD spectrum of the oxidized NO reductase were quite different. The strong derivative-shaped Soret bands were indicative of the presence of the low-spin hemes (Ookubo et al., 1987). On the other hand, the feature, + − + − sign bands in the Q band region indicated the presence of a high-spin heme. In addition, the ratio of the strength of the MCD bands for the Soret and the Q band regions was in the range for high- and low-spin hemes with a 1:2 ratio (Ookubo et al., 1987). All these low-spin heme features were not of the 5-coordinate heme but of the 6-coordinate heme. By taking these spectral features into consideration, we concluded that a low-spin heme *c*, a low-spin heme *b*, and a high-spin heme *b* are contained in the NO reductase.

The EPR spectrum of the oxidized NO reductase is shown in Figure 5. In the spectra measured at 7 K a high-spin heme and two low-spin hemes were observed. The former gave a split signal at $g = 6.6$ and 6.0 for a slightly distorted

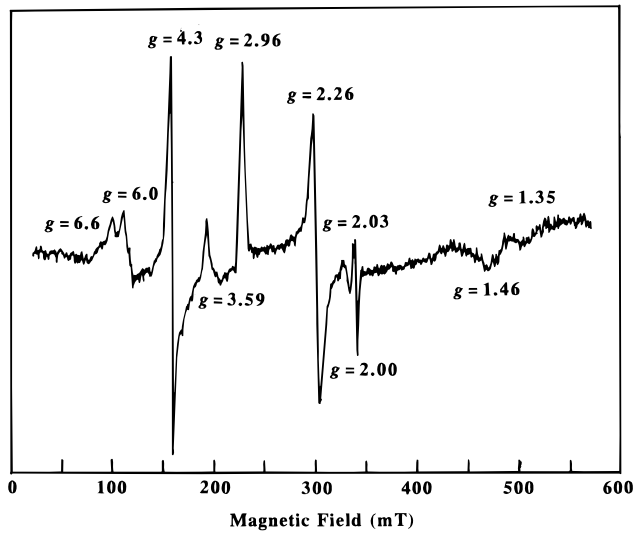

FIGURE 5: EPR spectra of NO reductase in the oxidized form measured at 7 K. The enzyme concentration was 1.5 mg/mL in 20 mM HEPES-NaOH buffer (pH 7.0) containing 0.05% *n*-dodecyl β-D-maltoside, 0.01% 2-phenylethanol, and 0.25 mM benzamidine. Instrument conditions: frequency 9.497 GHz, microwave power 5.1 mW, modulation frequency 100 kHz, modulation amplitude 0.96 mT, time constant 163 ms, and scan time 11 min.

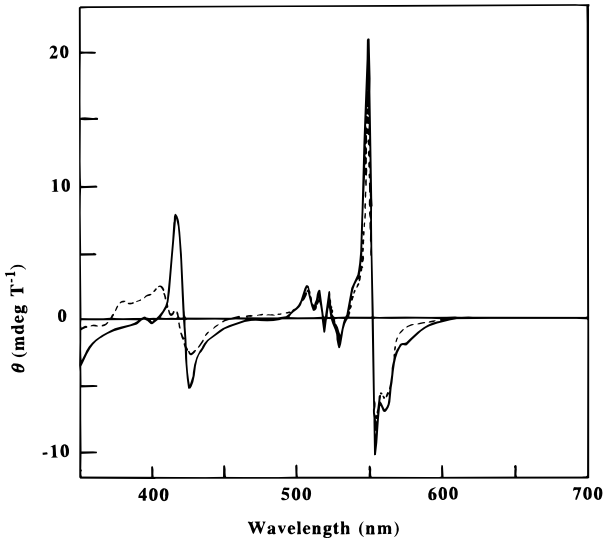

FIGURE 6: MCD spectra of CO- (solid line) and NO-acted (broken line) reduced NO reductase. The enzyme concentration was 0.109 mg/mL in 20 mM HEPES-NaOH buffer (pH 7.0) containing 0.05% *n*-dodecyl β-D-maltoside, 0.01% 2-phenylethanol, and 0.25 mM benzamidine.

octahedral geometry (Palmer, 1980). One of the latter hemes showed a rhombic signal with parameters $g_z = 2.96$, $g_y = 2.26$, and $g_x = 1.46$. Another low-spin heme could be detected only from its g_z component ($g_z = 3.59$) (g_y and g_x components might be at 2.03 and 1.35, respectively). Missing or difficulty to detect g_y and g_x signals might be caused by the highly rhombic character of this low-spin heme. A non-heme ion in a high-spin state might give a signal at ca. $g = 2.00$. However, it seemed to be coming from an adventitious nonmetallic radical judging from the microwave power dependency. Another signal at $g = 4.3$ could be derived from a very small amount of an adventitious non-heme iron.

When CO acted on the reduced NO reductase, the low-spin hemes were hardly affected, as was shown in the MCD spectrum for the Q band region (Figure 6). However, in the Soret band regions the MCD feature characteristic of the high-spin heme disappeared and the features of the new low-spin heme became more prominent. This indicates that CO was bound to the high-spin heme center with the possible concomitant change in the spin state. On the other hand, when NO acted on the reduced NO reductase, the intensities of the MCD bands in the Q band region were slightly decreased because the low-spin hemes *b* and *c* were partly oxidized (ca. 15%) by transferring electrons to NO; under the steady-state conditions, turnover takes place.

DISCUSSION

Nitric oxide reductase has been reported to be present in denitrifying bacteria *Ps. stutzeri* (Kastrau et al., 1994), *Ps. aeruginosa* (Arai et al., 1995a,b), *P. denitrificans* (formerly named *T. pantotropha*) (Carr & Ferguson, 1990; Fujiwara & Fukumori, 1996; Girsch & de Vries, 1997), *P. halodenitrificans* (Grant et al., 1984), *Rb. capsulatus* (Bell. et al., 1992), and *A. cycloclastes* (Jones & Hollocher, 1993). However, NO reductases have not been isolated from *P. halodenitrificans* and *A. cycloclastes* in the pure form and a few fractions of chromatography have been optically characterized. We found that the NO reductase of *P. halodenitrificans* can be completely purified by selecting the appropriate detergent and resin for the chromatographies. While a suitable detergent was found to differ from bacterium to bacterium as far as we screened for a large number of combinations of detergents and bacteria, *n*-dodecyl β-D-maltoside was extremely suitable to purify *P. halodenitrificans* NO reductase. The stability of this NO reductase in the presence of *n*-dodecyl β-D-maltoside is much higher than that of *Ps. stutzeri*, the best-characterized NO reductase. Further, among the many anion-exchange resins, DEAE-Toyopearl realized an extremely high resolution and the least loss of proteins during the chromatography (Figure 1). As for hydroxyapatite, the ceramic one showed an excellent resolution and satisfactory yield by minimizing smearing of NO reductase over the column (Figure 2). Thus, the structural, kinetic, and genetic studies of NO reductase from *P. halodenitrificans* have become possible (Table 1). In this paper the procedure for purification and basic spectroscopic characterization have been described.

SDS−PAGE (gradient gel of 15−25% acrylamide) showed two bands with apparent molecular masses of 20 and 42 kDa, representing the cytochrome *c* and *b* subunits, respectively (Figure 3). The molecular masses for the cytochrome *c* and *b* subunits reported hitherto are 15−18 and 34−38 kDa for the *P. denitrificans* enzyme (Carr & Ferguson, 1990; Dermastia et al., 1991; Fujiwara & Fukumori, 1996; Girsch & de Vries, 1997), 17 and 38 kDa for the *Ps. stutzeri* enzyme (Kastrau et al., 1994), and 17.5 and 38 kDa for the *A. cycloclastes* enzyme (Jones & Hollocher, 1993), respectively. The molecular masses of both cytochrome *c* and *b* subunits of *P. halodenitrificans* are the highest among those already identified (the apparent molecular mass of the cytochrome *b* subunit changed depending on the concentration of acrylamide; it appeared as 36 kDa on the gradient gel of 10−15% acrylamide). According to gene coding the molecular masses of the cytochrome *b* subunits have been revealed to be 52 and 53 kDa for those from *Ps. aeruginosa* (Arai et al., 1995a,b) and *Ps. stutzeri* (Jüngst & Zumft, 1992;

Zumft et al., 1994), respectively. This considerable discrepancy in molecular mass was caused by the fact that the cytochrome *b* subunit has 12 hydrophobic segments (Jüngst & Zumft, 1992; Arai et al., 1995a) and is not completely denatured by SDS or the hydrophobic regions are surrounded by more SDS than usual proteins. The cytochrome *c* subunit has been considered to exert an anchoring segment to interact with the cytochrome *b* subunit in the membrane. According to the sequence of the present NO reductase (in progress), the anchoring segment is appreciably conserved in comparison with those of *Ps. aeruginosa*, *Ps. stutzeri*, *P. denitrificans* (de Boer, et al., 1997), and *Rhodobacter sphaeroides* (Bartnikas et al., 1997). However, the sequence homologies for both of the N-termini in the cytochrome *b* and *c* subunits are only ca. 40−50%.

The analysis of the prosthetic group indicated a stoichiometry of 2 hemes *b* and 1 heme *c*, in agreement with the results for the *P. denitrificans* enzyme (Fujiwara & Fukumori 1996; Girsch & de Vries, 1997). The presence of an extra non-heme iron was suggested for the enzymes from *Ps. stutzeri* (Kastrau et al., 1994) and *P. denitrificans* (Fujiwara & Fukumori, 1996; Girsch & de Vries, 1997). Molecular evolution might have converted this non-heme binding site to bind copper in terminal oxidases, cytochrome oxidase, and ubiquinol oxidase in order to adapt for the change of substrate under aerobic conditions (Saraste & Castresana, 1994). If this is true, the non-heme iron to show the $g = 2.00$ or 4.3 EPR signal is not an adventitious iron but should play a crucial role in the NO reduction process. Girsch and de Vries (1997) assigned the signal from *P. denitrificans* at $g = 2.009$ as coming from a non-heme iron. However, differing from their results, our corresponding signal was not strong and saturated easily, suggesting that it originates in a nonmetallic radical. If a non-heme iron is four-coordinated and is in a tetrahedral environment, the $g = 4.3$ signal is more probable as coming from the non-heme iron. Although the protein molecule was denatured using guanidine hydrochloride or SDS−thioglycolate to ensure complete chelate formation for calorimetric determinations of non-heme iron, we did not obtain evidence whether an intrinsic non-heme iron is present or not in the NO reductase. Nevertheless, atomic absorption spectroscopy suggested the presence of the non-heme iron. As for this reason, NO reductase might not be completely denatured for titration because the non-heme iron is deeply buried inside the protein molecule. Alternatively, a portion of the non-heme iron might have been lost during preparation without affecting the enzyme activity. The sequence determination suggested the presence of a metal binding site.

Absorption, MCD, and EPR spectra (Figures 4 and 5) clearly showed the presence of three heme centers. Comparative inspection of the spectra was very effective for distinguishing these three heme centers. Heme *c* is apparently in the low-spin state as was evidenced by the absorption and MCD spectra, showing a peculiar α band at 552 nm in the reduced form. Two cytochromes *b* are in both the low- and high-spin states (Yamanaka, 1988). The low-spin heme *b* was distinguished by the α band at ca. 560 nm in the reduced form. Both of the low-spin heme centers are typical for the 6-coordinated ones; i.e., the apical positions are occupied by ligands that exert a strong ligand field. The α band due to the high-spin heme *b* was not clearly resolved

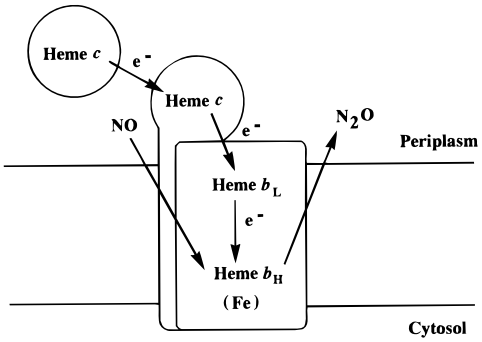

FIGURE 7: Proposal for the structure and function of NO reductase.

in the absorption spectrum for the reduced enzyme because it was broadened and was superimposed on the other bands. However, the broad band of the oxidized enzyme at around 595 nm was assigned as coming from the high-spin heme *b* (Makinen & Chung, 1983; Girsch & de Vries, 1997). Although it is not necessarily easy to quantify the EPR-detectable amount of heme signals, the signals ($g_\perp = 6.6$ and 6.0) with rhombic symmetry are derived from the high-spin heme *b*. Two low-spin heme centers gave the rhombic EPR signals. A set of *g* components ($g_{z,y,x} = 2.96$, 2.26, 1.46) was clearly resolved, being assigned to heme *c* with His and Met axial coordinations (Moore et al., 1985; Gadby et al., 1987). Only the $g_z = 3.59$ signal with higher anisotropy was observed as another low-spin heme (g_y and g_x components might be at 2.03 and 1.35, respectively). This type of resonance is characteristic of the so-called strong "g_{gem}" found for various low-spin hemes *b* with axial imidazole ligands (Walker et al., 1986). This spectral feature is very similar to that of the heme b_L center in the cytochrome bc_1 complex (de Vries & Albracht, 1979; McCurley et al., 1990), which has also two hemes *b* and a heme *c*.

When CO acted on the reduced NO reductase (Figure 6), the low-spin hemes were hardly affected, but the high-spin heme was influenced because the exogenous small molecule occupied an apical position that had been vacant or weakly coordinated by a water molecule. The binding of NO for this site also easily took place, since CO and also NO are classified as the strongest ligands for metal centers. The fact that both of the low-spin heme *b* and *c* centers were partly oxidized when NO acted on the reduced NO reductase (Figure 6) strongly suggests these low-spin heme centers function as electron donors. Although we have not yet determined the redox potential of the heme centers, Kastrau et al. (1994) reported that the redox potentials of cytochrome *b* (probably the mean value of two hemes *b*) and cytochrome *c* in *Ps. stutzeri* NO reductase are +322 and +280 mV, respectively. Thus cytochrome *c* is found to be the potential electron donor to cytochrome *b*. The soluble cytochrome *c*, which has the lower redox potential (Sakurai et al., 1997), has been postulated to function as the electron donor toward NO reductase in the biological system (Fujiwara & Fukumori, 1996).

In conclusion, Figure 7 depicts the simplified structure and function of NO reductase. More detailed spectroscopic and sequencing studies are in progress to reach to a profound understanding of NO reductase. Since it is apparent that NO reductase shows cytochrome oxidase activity, an evolutionary study should be performed in addition to structural and kinetic studies.

ACKNOWLEDGMENT

Special thanks are due to Professor W. G. Zumft of Universität Karlsruhe for the supply of *Pseudomonas stutzeri* and Dr. Tetsuhiko Yoshimura of the Institute for Life Support Technology, Yamagata Technopolis Foundation, for interpretation of the spectra. We also thank Mr. Hong-wei Huang of our research group for his technical assistance to measure EPR spectra. N.S. has been encouraged by Professor Tatsuya Samejima of Aoyamagakuin University throughout this study.

REFERENCES

Arai, H., Igarashi, Y., & Kodama, T. (1995a) *Biochim. Biophys. Acta 1261*, 279−284.

Arai, H., Igarashi, Y., & Kodama, T. (1995b) *FEBS Lett. 371*, 73−76.

Antholine, W. E., Kastrau, D. H. W., Steffens, G. C. M., Buse, G., Zumft, W. G., & Kroneck, P. M. H. (1992) *Eur. J. Biochem. 209*, 875−881.

Averill, B. A. (1996) *Chem. Rev. 96*, 2951−2964.

Averill, B. A., & Tiedje, J. M. (1982) *FEBS Lett. 138*, 8−12.

Bartnikas, T. B., Tosgues, I. E., Laratta, W. P., Shi, J., & Shapleigh, J. P. (1997) *J. Bacteriol. 179*, 3534−3540.

Bell, L. C., & Ferguson, S. J. (1991) *Biochem. J. 273*, 423−427.

Bell, L. C., Richardson, D. J., & Ferguson, S. J. (1992) *J. Gen. Microbiol. 138*, 437−443.

Berks, B. C., Richardson, D. J., Robinson, C., Reilly, A., Aplin, T., & Ferguson, S. J. (1994) *Eur. J. Biochem. 220*, 117−124.

Berks, B. C., Ferguson, S. J., Moir, J. W. B., & Richardson, D. J. (1995*) Biochim. Biophys. Acta 1232*, 97−173.

Berry, E. A., & Trumpower, B. L. (1987) *Anal. Biochem. 161*, 1−15.

de Boer, A. P. N., Reijnders, W. N. M., Stouthamer, A. H., & van Spanning, R. J. M. (1997) NCIB GenBank U28078.

Carr, G. J., Page, M. D., & Ferguson, S. J. (1989) *Eur. J. Biochem. 179*, 683−692.

Carr, G. J., & Ferguson, S. J. (1990) *Biochem. J. 269*, 423−429.

Dermastia, M., Turk, T., & Hollocher, T. C. (1991) *J. Biol. Chem. 266*, 10899−10905.

de Vries, S., & Albracht, S. P. J. (1979) *Biochim. Biophys. Acta 546*, 334−340.

DiSpirito, A. A. (1990) *Methods Enzymol. 188*, 289−297.

Frunzke, K., & Zumft, W. G. (1984) *J. Chromatogr. 299*, 477−483.

Fujiwara, T., & Fukumori, Y. (1996) *J. Bacteriol. 178*, 1866−1871.

Gadsby, P. M. A., Peterson, J., Foote, N., Greenwood, C., & Thomson, A. J. (1987) *Biochem. J. 246*, 43−54.

Girsch, P., & de Vries, S.(1997) *Biochim. Biophys. Acta 1318*, 202−216.

Godden, J. W., Turley, S., Teller, D. C., Adman, E. T., Liu, M. Y., Payne, W. J., & LeGall, J. (1991) *Science 253*, 438−442.

Grant, M. A., Cronin, S. E., & Hochstein, L. I. (1984) *Arch. Microbiol. 140*, 183−186.

Heiss, B., Frunzke, K., & Zumft, W. (1989) *J. Bacteriol. 171*, 3288−3297.

Hennessy, D. J., Reid, G. R., Smith, F. E., & Thompson, S. L. (1984) *Can. J. Chem. 62*, 721−724.

Jones, A. M., & Hollocher, T. C. (1993) *Biochim. Biophys. Acta 1144*, 359−366.

Jüngst, A., & Zumft, W. G. (1992) *FEBS Lett. 314*, 308−314.

Kastrau, D. H. W., Heiss, B., Kroneck, P. H. M., & Zumft, W. G. (1994) *Eur. J. Biochem. 222*, 293−303.

Lu, G., Lindqvist, Y., Schneider, G., Dwivedi, U., & Campbell, W. (1995) *J. Mol. Biol. 248*, 931−948.

Makinen, M. W., & Chung, A. K. (1983) in *Iron Porphyrins* (Lever, A. B. P., & Gray, H. B., Eds.) Part 1, pp. 141−236, Addison-Wesley, London.

Makino, T., Kiyonaga, M., & Kina, K. (1988) *Clin. Chim. Acta 171*, 19−38.

Masuko M., Iwasaki, H., Sakurai, T., Suzuki, S., & Nakahara, A. (1984) *J. Biochem. (Tokyo) 96*, 447−454.

Matsubara, T., & Iwasaki, H. (1971) *J. Biochem. (Tokyo) 69*, 859−868.

Matsubara, T., & Zumft, W. G. (1982) *Arch. Microbiol.* 132, 322−328.

Matsubara, K., Shinagawa, E., Adachi, O., & Ameyama, M. (1982) *FEBS Lett. 139*, 255−258.

McCurley, J. P., Miki, T., Yu, L., & Yu, C. (1990) *Biochim. Biophys. Acta 1020*, 176−186.

Moir, J. W. B., Baratta, D., Richardson, D., & Ferguson, S. J. (1993) *Eur. J. Biochem. 212*, 377−385.

Moore, G. R., Williams., R. J. P., Peterson, J., Thomson, A. J., & Mathews, F. S. (1985) *Biochim. Biophys. Acta 829*, 83−96.

Ookubo, S., Nozawa, T., & Hatano, M. (1987) *J. Inorg. Biochem. 30*, 45−68.

Palmedo, G., Seither, P., Körner, H., Matthews, J. C., Burkhalter, R. S., Timkovich, R., & Zumft, W. G. (1995) *Eur. J. Biochem. 232*, 737−746.

Palmer, G. (1980) in *Methods for Determining Metal Ion Environments in Proteins: Structure and Function of Metalloproteins* (Darnall, D. W., & Wilkins, P. G., Eds.) pp 153−182, Elsevier, New York.

Sakurai, N, Kumita, H., Sakurai, T., & Masuda, H. (1997) *Bull. Chem. Soc. Jpn.* (submitted for publication).

Saraste, M., & Castresana, J. (1994) *FEBS Lett. 341*, 1−4.

Shiro, Y., Fujii, M., Iizuka, T., Adachi, S., Nakahara, K., & Shoun, H. (1995) *J. Biol. Chem. 270*, 1617−1623.

Turk, T., & Hollocher, T. C. (1992) *Biochem. Biophys. Res. Commun. 183*, 983−988.

Walker, F. A., Huynh, B. H., Scheidt, W. R., & Osvath, S. R. (1986) *J. Am. Chem. Soc. 108*, 5288−5297.

Yamanaka, T. (1988) in *Metalloproteins, Chemical Properties and Biological Effects* (Otsuka, S., & Yamanaka, S., Eds.) pp. 134−139, Kodansha, Tokyo, and Elsevier, Amsterdam.

Yamazaki, T., Oyanagi, H., Fujiwara, T., & Fukumori, Y. (1995) *Eur. J. Biochem. 233*, 665−671.

Zimmer, W., Danneberg, G., & Bothe, H. (1985) *Curr. Microbiol. 12*, 341−346.

Zumft, W. G., & Vega, J. M. (1979) *Biochim. Biophys. Acta 548*, 484−499.

Zumft, W. G., & Frunzke, K. (1982) *Biochim. Biophys. Acta 681*, 459−468.

Zumft, W. G., Braun, C., & Cuypers, H. (1994) *Eur. J. Biochem. 219*, 481−490.

BI971070U